# Integral cross sections for electron scattering by ground-state Ba atoms

D. V. Fursa,[1,*] S. Trajmar,[2] I. Bray,[1] I. Kanik,[2] G. Csanak,[3] R. E. H. Clark,[3] and J. Abdallah, Jr.[3]
[1]*The Flinders University of South Australia, G.P.O. Box 2100, Adelaide 5001, Australia*
[2]*Jet Propulsion Laboratory, California Institute of Technology, Pasadena, California 91109*
[3]*Los Alamos National Laboratory, University of California, Los Alamos, New Mexico 87545*
(Received 10 June 1999)

We have used the convergent close-coupling method and a unitarized first-order many-body theory to calculate integral cross sections for elastic scattering and momentum transfer, for excitation of the $5d^2\,{}^1S$, $6s6p\,{}^1P_1$, $6s7p\,{}^1P_1$, $6s8p\,{}^1P_1$, $6s5d\,{}^1D_2$, $5d^2\,{}^1D_2$, $6s6d\,{}^1D_2$, $6p5d\,{}^1F_3$, $6s4f\,{}^1F_3$, $6p5d\,{}^1D_2$, $6s6p\,{}^3P_{0,1,2}$, $6s5d\,{}^3D_{1,2,3}$, and $6p5d\,{}^3D_2$ states, for ionization and for total scattering by electron impact on the ground state of barium at incident electron energies from 1 to 1000 eV. These results and all available experimental data have been combined to produce a recommended set of integral cross sections.
[S1050-2947(99)02912-1]

PACS number(s): 34.80.Bm, 34.80.Dp

## I. INTRODUCTION

A great deal of interest and need has developed in recent years for electron collision cross sections involving Ba atoms. In the applications area, these cross sections are needed for modeling the behavior of Ba vapor lasers [1–4], discharge lamps [5], plasma switches [6], and various planetary ionospheres [7–12], where Ba has often been used as a trace element for diagnostic purposes. On the academic side, benchmark laboratory cross sections are needed for testing various theoretical approximations and calculational methods hoping to predict these cross sections.

The experimental database, available at the present time, is rather limited both in the electron impact energy range and the scattering channels. Line emission cross sections for the $(6s6p\,{}^1P_1 \rightarrow 6s^2\,{}^1S)$ at 5535 Å $[Q_{\rm emiss}(6s6p\,{}^1P_1)]$ were determined by Chen and Gallagher [13] in the 2.3–1497.0-eV impact energy range. They claimed an uncertainty of $\pm 5\%$. Since the $6s6p\,{}^1P_1$ level decays predominantly (99.7%) to the ground state, the measured line emission cross sections are equivalent (within the experimental error limits) to the apparent $6s6p\,{}^1P_1$ level excitation cross sections $[Q_{\rm app}(6s6p\,{}^1P_1)]$ and they differ from the electron impact excitation cross sections $[Q(6s6p\,{}^1P_1)]$ by the cascade contributions. (See, e.g., Trajmar and Nickel [14] for the definitions of these cross sections.) Cascade corrections, only available from theory, can be applied to the data of Chen and Gallagher, and the resulting $Q(6s6p\,{}^1P_1)$ values represent the most reliable electron scattering cross sections available for Ba at the present time [15]. Jensen *et al.* [16] and Wang *et al.* [17] determined relative cross sections for elastic scattering ($Q_{\rm elas}$) and momentum transfer ($Q_M$) at a few impact energies. Jensen *et al.* [16] also obtained some cross-section results for excitation of the $6s5d\,{}^1D_2$ level $[Q(6s5d\,{}^1D_2)]$. In these cases, the relative cross sections were normalized by an estimated cascade correction applied to the Chen and Gallagher $Q_{\rm app}(6s6p\,{}^1P_1)$ values to obtain $Q(6s6p\,{}^1P_1)$ values which in turn were used to normalize $Q_{\rm elas}$, $Q_M$, and $Q(6s5d\,{}^1D_2)$. Total ionization cross sections ($Q_i$) in the threshold to 600 eV range have been reported by Dettmann and Karstensen [18] and by Vainshtein *et al.* [19] from the threshold to 200 eV. Total electron scattering cross sections ($Q_{\rm tot}$) were measured by Romanyuk *et al.* [20] in the 0.1–10-eV range.

There is a larger database available from calculations. Elastic-scattering cross sections were calculated by Gregory and Fink [21] in the 100–1500-eV range (numerical solutions of the Dirac equation), by Fabrikant [22] at impact energies ranging from 6 to 35 eV (nonrelativistic close-coupling approximation), by Yuan and Zhang from 0.01 to 5.0 eV (quasirelativistic static-exchange formalism) [23] and from 0.04 to 150 eV (Hartree-Fock method with relativistic corrections) [24], by Szmytkowski and Sienkiewicz [25] in the 0.2–100-eV region (relativistic polarized-orbital approximation), and by Kelemen *et al.* [26] from 0.1 to 200 eV (using the phenomenological complex opical potential). Szmytkowski and Sienkiewicz [25] and Kelemen *et al.* [26] as well as Gribakin *et al.* [27] (Hartree-Fock approximation with correlation corrections, from zero to 2.5 eV) have reported momentum transfer cross sections. As far as inelastic scattering is concerned, $Q(6s6p\,{}^1P_1)$ results were obtained by Fabrikant [22] from threshold to 35 eV (nonrelativistic two-state close-coupling approximation), by Clark *et al.* [28] from 5 to 100 eV [unitarized distorted-wave approximation (UDWA) and unitarized first-order many-body theory (UFOMBT)], and Srivastava *et al.* [29,30] from 20 to 100 eV [relativistic distorted-wave approximation (RDWA)]. Srivastava *et al.* also reported $Q(6s6p\,{}^3P_1)$ and $Q(6s5d\,{}^1D_2)$ and $Q(6s5d\,{}^3D_{1,2,3})$ values. $Q_{\rm tot}$ results in the 10–200-eV range were given by Kelemen *et al.* [26]. Very recently the nonrelativistic convergent close-coupling (CCC) method was applied by Fursa and Bray [31,15] to obtain $Q_{\rm elas}$, $Q_M$, $Q(6s6p\,{}^3P_1)$, $Q(6s5d\,{}^1D_2)$, and $Q_{\rm app}(6s6p\,{}^1P_1)$ results in the 1–897-eV range.

The present work represents a substantial extension of CCC and UFOMBT calculations to cover all scattering channels which we consider important for practical applications over a wide range of impact energies. Comparison of these theoretical results with fragmentary experimental data allows

*Electronic address: dmitry.fursa@flinders.edu.au

 

TABLE I. Excitation energies and dominant configurations for the barium levels from CCC and CC(55) nonrelativistic calculations. The experimental data are from Refs. [37] and [38] ($5d^2\,{}^1S$ level). States are labeled by the major configuration.

| Experiment | | Present | | |
|---|---|---|---|---|
| Label | $E$ (eV) | Label | $E$ (eV) | Dominant configurations |
| $6s^2\,{}^1S$ | 0.00 | $6s^2$ | 0.00 | $0.944(6s^2\,{}^1S)+0.228(6p^2\,{}^1S)-0.191(7s6s\,{}^1S)$ |
| $5d^2\,{}^1S$ | 3.32 | $5d^2$ | 3.34 | $0.591(7s6s\,{}^1S)-0.519(5d^2\,{}^1S)+0.369(nd5d\,{}^1S)$ |
| $6s6p\,{}^1P$ | 2.24 | $6s6p$ | 2.27 | $0.800(6p6s\,{}^1P)-0.504(5d6p\,{}^1P)$ $-0.256(7p6s\,{}^1P)$ |
| $6s7p\,{}^1P$ | 3.54 | $6s7p$ | 3.62 | $0.688(7p6s\,{}^1P)-0.550(5d6p\,{}^1P)$ $+0.331(5d7p\,{}^1P)$ |
| $6s8p\,{}^1P$ | 4.04 | $6s8p$ | 4.14 | $0.788(6snp\,{}^1P)+0.301(5d6p\,{}^1P)$ $-0.505(5d7p\,{}^1P)$ |
| $6s5d\,{}^1D$ | 1.41 | $6s5d$ | 1.44 | $0.896(5d6s\,{}^1D)-0.226(5d7s\,{}^1D)-0.226(5d^2\,{}^1D)$ |
| $5d^2\,{}^1D$ | 2.86 | $5d^2$ | 3.04 | $0.798(5d^2\,{}^1D)-0.442(nd5d\,{}^1D)+0.350(6p^2\,{}^1D)$ |
| $6s6d\,{}^1D$ | 3.75 | $6s6d$ | 3.79 | $0.893(nd6s\,{}^1D)-0.369(5d7s\,{}^1D)-0.162(6p^2\,{}^1D)$ |
| $5d6p\,{}^1D$ | 2.86 | $5d6p$ | 2.87 | $0.946(5d6p\,{}^1D)-0.289(5d7p\,{}^1D)$ |
| $5d6p\,{}^1F$ | 3.32 | $5d6p$ | 3.35 | $0.852(5d6p\,{}^1F)-0.424(5d7p\,{}^1F)$ $+0.280(nf6s\,{}^1F)$ |
| $6s4f\,{}^1F$ | 4.31 | $6s4f$ | 4.36 | $0.973(nf6s\,{}^1F)+0.165(5d7p\,{}^1F)$ $-0.141(nd6p\,{}^1F)$ |
| $6s6p\,{}^3P$ | 1.62 | $6s6p$ | 1.59 | $0.960(6p6s\,{}^3P)-0.161(5d6p\,{}^3P)$ $-0.116(6p7s\,{}^3P)$ |
| $5d6p\,{}^3P$ | 3.20 | $5d6p$ | 3.30 | $0.873(5d6p\,{}^3P)-0.394(5d7p\,{}^3D)$ $-0.215(7p6s\,{}^3P)$ |
| $5d^2\,{}^3P$ | 2.94 | $5d^2$ | 3.11 | $0.799(5d^2\,{}^3P)+0.458(nd5d\,{}^3D)+0.389(6p^2\,{}^3P)$ |
| $6s5d\,{}^3D$ | 1.16 | $6s5d$ | 1.21 | $0.955(5d6s\,{}^3D)-0.201(5d7s\,{}^3D)$ $-0.112(nf6p\,{}^3D)$ |
| $6s6d\,{}^3D$ | 3.85 | $6s6d$ | 3.82 | $0.961(nd6s\,{}^3D)-0.208(5d7s\,{}^3D)$ |
| $5d6p\,{}^3D$ | 3.06 | $5d6p$ | 3.12 | $0.924(5d6p\,{}^3D)-0.361(5d7p\,{}^3D)$ |
| $5d6p\,{}^3F$ | 2.86 | $5d6p$ | 2.88 | $0.934(5d6p\,{}^3F)-0.289(5d7p\,{}^3F)$ $+0.129(nf6s\,{}^3F)$ |

us to recommend a reliable and consistent cross-section data set, which should be satisfactory for most modeling calculations. We found very good agreement between the CCC results and experiment, and therefore in our recommendations we relied heavily on the CCC data.

## II. CALCULATIONAL METHODS

### A. CCC method

The application of the CCC method to calculation of electron scattering from barium has been discussed elsewhere, see Refs. [15] and [32] for details. Briefly, barium target states are described by a model of two valence electrons above an inert Hartree-Fock core. We have used a configuration-interaction (CI) expansion technique to obtain barium wave functions. One-electron orbitals used in the CI expansion have been obtained by diagonalizing a $Ba^+$ Hamiltonian in a Sturmian (Laguerre) basis. One- and two-electron core-polarization potentials have been added to improve agreement with experimental energy levels and optical oscillator strength. In Table I we compare energies for the states relevant to the present study with experimental data and give a set of the dominant configurations for each state. We find very good agreement between our results and experiment and other accurate calculations for energy levels and oscillator strengths [15]. The barium target states obtained in this way provide not only an accurate representation of the barium discrete spectrum but also allow for a square-integrable representation of the target continuum. This allows for coupling to the ionization channels in the scattering calculations. These calculations use barium target states in order to perform an expansion of the total wave function and formulate a set of close-coupling equations. These equations (for the $T$ matrix) are formulated and solved in momentum space.

We have performed $e$-Ba scattering calculations using two models [15]. In the first model, we have performed 55-state close-coupling calculations [CC(55)] where only barium discrete spectrum states have been included in the close-coupling expansion. In the second model, we have performed 115-state close-coupling calculations (CCC). The close-coupling expansion in this case includes a large number of positive energy states (relative to the $Ba^+$ ground state) which allow us to model coupling to the ionization channels. The difference between CC(55) and CCC results is expected to reveal the relative importance of the ionization channels.

The CCC method is formulated as a purely nonrelativistic theory in both target structure and electron scattering calculations. In order to compare results from the nonrelativistic

CCC calculations with experiment, we have used a technique essentially identical with the transformation scheme described by Saraph [33]. Namely, we first transform the nonrelativistic CCC scattering amplitudes $f^{S}_{\pi_f s_f l_f m_f,\pi_i s_i l_i m_i}$ to the amplitudes describing transitions between fine-structure levels $J_f$ and $J_i$,

$$f^{\sigma_f,\sigma_i}_{\pi_f J_f M_f,\pi_i J_i M_i}(s_f l_f \gamma_f, s_i l_i \gamma_i) = \sum_{m_f,q_f,m_i,q_i,S} C^{J_f M_f}_{l_f m_f, s_f q_f} C^{S M_S}_{(1/2)\sigma_f, s_f q_f} \times C^{J_i M_i}_{l_i m_i, s_i q_i} C^{S M_S}_{(1/2)\sigma_i, s_i q_i} f^{S}_{\pi_f s_f l_f m_f,\pi_i s_i l_i m_i}(\gamma_f,\gamma_i). \quad (1)$$

Here $S$ is the total spin, and $\pi_f$ ($\pi_i$), $s_f$ ($s_i$), $l_f$ ($l_i$), and $m_f$ ($m_i$) are the final (initial) target state parity, spin, orbital angular momentum, and its projection on the $Z$ axis of the collision frame, respectively. The final (initial) projectile spin projection on the $Z$ axis of the collision frame is indicated as $\sigma_f$ ($\sigma_i$), and the index $\gamma$ distinguishes states with the same orbital angular momentum, spin, and parity. The above amplitudes are used to form amplitudes in the intermediate coupling scheme

$$F^{\sigma_f,\sigma_i}_{\pi_f J_f M_f,\pi_i J_i M_i}(\beta_f,\beta_i) = \sum_{s_f,l_f,s_i l_i} \sum_{\gamma_f,\gamma_i} C^{\beta_f}_{\gamma_f} C^{\beta_i}_{\gamma_i} f^{\sigma_f,\sigma_i}_{\pi_f J_f M_f,\pi_i J_i M_i}(s_f l_f \gamma_f, s_i l_i \gamma_i), \quad (2)$$

where the index $\beta$ distinguishes target states with the same total angular momentum $J$ and parity $\pi$. We obtain mixing coefficients $C^{\beta}_{\gamma}$ by diagonalizing the Breit-Pauli Hamiltonian (only the one-body spin-orbit term is used) in the basis of the barium target states obtained from the nonrelativistic barium structure calculation. Note that the dependence of the scattering amplitudes in Eqs. (1) and (2) on the electron spherical angles $\theta$ and $\varphi$ is implicit.

Amplitudes (2) are used to calculate the semirelativistic integrated cross sections:

$$Q_{\mathrm{fs}} = \frac{k_f}{2(2J_i+1)k_i} \times \sum_{M_f,M_i,\sigma_f,\sigma_i} \int d\Omega |F^{\sigma_f,\sigma_i}_{\pi_f J_f M_f,\pi_i J_i M_i}(\beta_f,\beta_i)|^2. \quad (3)$$

The subscript ''fs'' (fine-structure) indicates that the cross section is calculated with an (approximate) account of relativistic corrections.

Scattering on a singlet initial state allows for significant simplification in Eq. (3). Symmetry relations of the scattering amplitudes (1),

$$f^{\sigma_f,\sigma_i}_{\pi_f J_f M_f,\pi_i J_i M_i}(s_f l_f \gamma_f, s_i l_i \gamma_i) = -(-1)^{s_f} f^{-\sigma_f,-\sigma_i}_{\pi_f J_f M_f,\pi_i J_i M_i}(s_f l_f \gamma_f, s_i l_i \gamma_i), \quad s_i = 0, \quad (4)$$

ensure that the singlet-triplet (interference) terms in Eq. (3) are zero after summation over projectile spin magnetic sublevels $\sigma_f$ and $\sigma_i$. We have also found that for the target states involved in the present study, only one or two terms in Eq. (2) have large mixing coefficients. Together, these allow us to express the cross section defined by Eq. (3) in terms of the nonrelativistic cross sections $Q$ which are obtained from the nonrelativistic amplitudes (1). We give below a decomposition of the semirelativistic ICS (3) via nonrelativistic cross sections,

$$Q_{\mathrm{fs}}(5d^2\,{}^1S) = 0.9635\,Q(5d^2\,{}^1S) + 0.0339\,Q(5d^2\,{}^3P_0), \quad (5a)$$

$$Q_{\mathrm{fs}}(6s6p\,{}^3P_1) = 0.9934\,Q(6s6p\,{}^3P_1) + 0.0058\,Q(6s6p\,{}^1P), \quad (5b)$$

$$Q_{\mathrm{fs}}(6s5d\,{}^1D_2) = 0.9779\,Q(6s5d\,{}^1D_2) + 0.0220\,Q(6s5d\,{}^3D_2), \quad (5c)$$

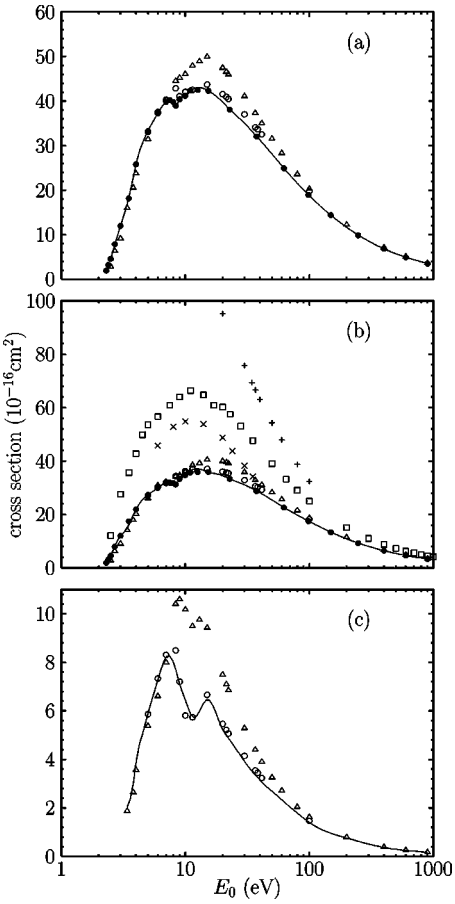


FIG. 1. Excitation of the $6s6p\,{}^1P_1$ level. (a) Apparent and (b) direct integral excitation cross sections, (c) cascade contribution to the apparent excitation cross section. Calculations are ○, CCC; △, CC(55); ×, CC(2), Fabrikant [22]; +, RDWA, Srivastava *et al.* [29]. Experimental data are ●, Chen and Galagher [13]. For the direct excitation cross section, the present theoretical estimate of the cascade contribution is subtracted from the apparent cross section of Chen and Galagher [13]. The solid line represents our recommended values.

TABLE II. Recommended values for $Q_{app}(6s6p\ ^1P_1)$, $Q_{cascade}(6s69\ ^1P_1)$, and $Q(6s6p\ ^1P_1)$ in units of $10^{-16}\,cm^2$.

| $E_0$ (eV) | $Q_{app}(6s6p\ ^1P_1)$ | $Q_{cascade}/Q_{app}$ (%) | $Q_{cascade}(6s6p\ ^1P_1)$ | $Q(6s6p\ ^1P_1)$ |
|---|---|---|---|---|
| 2.50 | 4.56 | 0.00 | 0.00 | 4.56 |
| 3.00 | 12.00 | 0.00 | 0.00 | 12.00 |
| 4.00 | 25.84 | 15.54 | 4.02 | 21.83 |
| 5.00 | 33.34 | 17.71 | 5.90 | 27.43 |
| 6.00 | 37.26 | 19.52 | 7.27 | 29.98 |
| 7.00 | 39.89 | 20.61 | 8.22 | 31.67 |
| 8.35 | 39.00 | 19.80 | 7.72 | 31.28 |
| 9.00 | 40.44 | 17.53 | 7.09 | 33.35 |
| 10.00 | 41.24 | 15.63 | 6.45 | 34.79 |
| 11.44 | 42.56 | 13.48 | 5.74 | 36.82 |
| 15.00 | 42.47 | 15.23 | 6.47 | 36.00 |
| 20.00 | 39.78 | 13.14 | 5.23 | 34.55 |
| 30.00 | 35.01 | 11.19 | 3.92 | 31.09 |
| 36.67 | 32.39 | 10.38 | 3.36 | 29.03 |
| 41.44 | 30.78 | 9.94 | 3.06 | 27.72 |
| 50.00 | 28.11 | 9.57 | 2.69 | 25.42 |
| 60.00 | 25.49 | 9.15 | 2.33 | 23.16 |
| 80.00 | 21.55 | 8.30 | 1.79 | 19.76 |
| 100.00 | 18.75 | 7.44 | 1.40 | 17.35 |
| 200.00 | 11.65 | 6.56 | 0.76 | 10.88 |
| 400.00 | 6.81 | 5.46 | 0.37 | 6.44 |
| 600.00 | 4.92 | 5.17 | 0.25 | 4.66 |
| 897.60 | 3.52 | 4.91 | 0.17 | 3.35 |

$$Q_{fs}(6s5d\ ^3D_2) = 0.9779\,Q(6s5d\ ^3D_2) + 0.0220\,Q(6s5d\ ^1D_2), \quad (5d)$$

$$Q_{fs}(6s6d\ ^1D_2) = 0.9845\,Q(6s6d\ ^1D_2) + 0.0136\,Q(6s6d\ ^3D_2), \quad (5e)$$

$$Q_{fs}(5d^2\ ^1D_2) = 0.8591\,Q(5d^2\ ^1D_2) + 0.1292\,Q(5d^2\ ^3P_2), \quad (5f)$$

$$Q_{fs}(6p5d\ ^1D_2) = 0.7774\,Q(6p5d\ ^1D_2) + 0.2091\,Q(6p5d\ ^3F_2), \quad (5g)$$

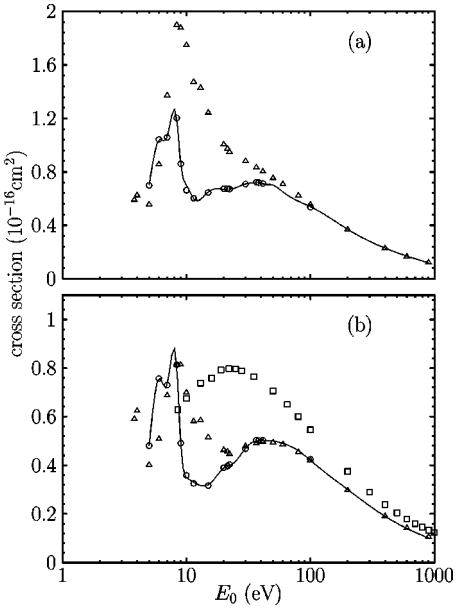


FIG. 2. Same as Fig. 1 except for the $6s7p\ ^1P_1$ level.

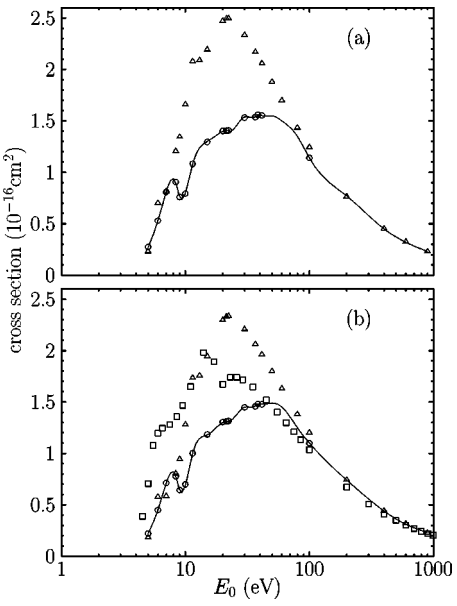


FIG. 3. Same as Fig. 1 except for the $6s8p\ ^1P_1$ level.

TABLE III. Recommended $Q(6s7p\ ^1P_1)$, $Q_{app}(6s7p\ ^1P_1)$, $Q(6s8p\ ^1P_1)$, and $Q_{app}(6s8p\ ^1P_1)$ values in units of $10^{-16}$ cm$^2$.

| $E_0$ (eV) | $Q(6s7p\ ^1P_1)$ | $Q_{app}(6s7p\ ^1P_1)$ | $Q(6s8p\ ^1P_1)$ | $Q_{app}(6s8p\ ^1P_1)$ |
|---|---|---|---|---|
| 5.00 | 0.48 | 0.70 | 0.22 | 0.27 |
| 6.00 | 0.76 | 1.04 | 0.45 | 0.53 |
| 7.00 | 0.73 | 1.06 | 0.71 | 0.81 |
| 8.35 | 0.81 | 1.20 | 0.78 | 0.90 |
| 9.00 | 0.49 | 0.86 | 0.64 | 0.76 |
| 10.00 | 0.35 | 0.70 | 0.69 | 0.80 |
| 11.44 | 0.33 | 0.60 | 1.00 | 1.08 |
| 15.00 | 0.32 | 0.65 | 1.18 | 1.30 |
| 20.00 | 0.39 | 0.67 | 1.30 | 1.40 |
| 30.00 | 0.47 | 0.71 | 1.45 | 1.54 |
| 36.67 | 0.50 | 0.72 | 1.46 | 1.54 |
| 41.44 | 0.50 | 0.71 | 1.48 | 1.55 |
| 50.00 | 0.50 | 0.70 | 1.49 | 1.55 |
| 60.00 | 0.49 | 0.65 | 1.45 | 1.50 |
| 80.00 | 0.46 | 0.58 | 1.25 | 1.35 |
| 100.00 | 0.42 | 0.54 | 1.10 | 1.14 |
| 200.00 | 0.30 | 0.37 | 0.74 | 0.77 |
| 400.00 | 0.19 | 0.23 | 0.44 | 0.45 |
| 600.00 | 0.14 | 0.17 | 0.31 | 0.32 |
| 897.60 | 0.10 | 0.12 | 0.23 | 0.23 |

$$Q_{fs}(6p5d\ ^3D_2) = 0.9878\, Q(6p5d\ ^3D_2) + 0.0075\, Q(6p5d\ ^1D_2), \quad (5h)$$

$$Q_{fs}(6p5d\ ^1F_3) = 0.9698\, Q(6p5d\ ^1F_3) + 0.0291\, Q(6p5d\ ^3D_3). \quad (5i)$$

These cross sections typically differ by less than 3% from the corresponding cross sections obtained from Eq. (3). All other target states are well described in the nonrelativistic approximation.

### B. UFOMBT method

The UFOMBT method used here has been discussed in general and in particular its implementation for Ba by Clark *et al.* [28] and Zetner *et al.* [34].

## III. RESULTS AND DISCUSSION

### A. Line emission, apparent level excitation, and electron impact excitation cross section for the $6s6p\ ^1P_1$ level

At the present time, the most reliable electron collision cross sections for Ba are the 5535-Å line emission cross sections $[Q_{emiss}(6s6p\ ^1P_1)]$ associated with the radiative decay of the electron impact and cascade populated $6s6p\ ^1P_1$ level to the ground $6s^2\ ^1S$ state as measured by Chen and Gallagher [13]. The uncertainty claimed for these cross sections is about ±5% over the 2.3 –1497-eV impact energy range. As mentioned in the Introduction, for all practical purposes these emission cross sections are equivalent to the apparent level excitation cross sections $[Q_{app}(6s6p\ ^1P_1)]$ from which the electron impact excitation cross sections $[Q(6s6p\ ^1P_1)]$ can be derived if proper account of the cascade contributions can be taken. These cross sections can be used as standards to normalize other electron collision cross sections obtained from relative measurements. Indeed, this procedure was followed by Jensen *et al.* [16] and Wang *et al.* [17], who assumed very approximate cascade contributions. A better estimate of these cascade contributions can be made based on the CCC calculations. We will follow here this latter procedure. In Fig. 1(a), the $Q_{app}(6s6p\ ^1P_1)$ values measured by Chen and Gallagher and those obtained from the CCC and CC(55) calculations (by adding the direct and cascade contributions) are shown. Figure 1(c) shows the cal-

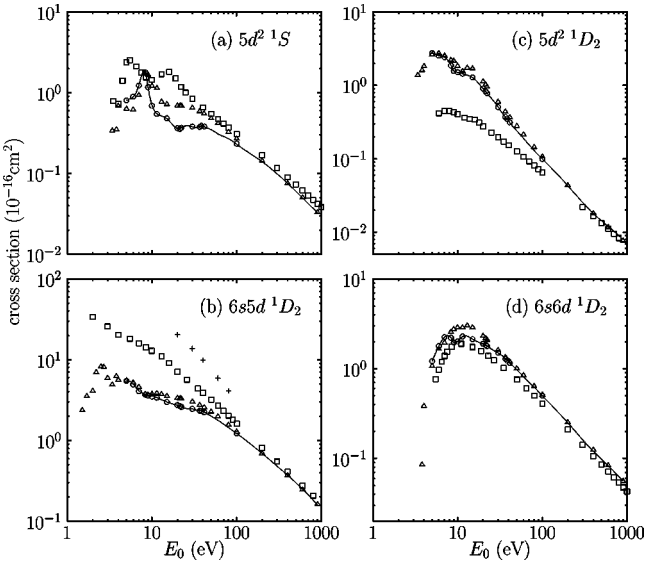


FIG. 4. Integral cross sections for excitation of (a) $5d^2\ ^1S$, (b) $6s5d\ ^1D_2$, (c) $5d^2\ ^1D_2$, and (d) $6s6d\ ^1D_2$ levels. Calculations are ○, CCC; △, CC(55); □, UFOMBT; +, RDWA, Srivastava *et al.* [30]. The solid line represents our recommended values.

TABLE IV. Recommended $Q(5d^2\,{}^1S)$, $Q(6s5d\,{}^1D_2)$, $Q(5d^2\,{}^1D_2)$, and $Q(6s6d\,{}^1D_2)$ values in units of $10^{-16}\,\mathrm{cm}^2$.

| $E_0$ (eV) | $Q(5d^2\,{}^1S)$ | $Q(6s5d\,{}^1D_2)$ | $Q(5d^2\,{}^1D_2)$ | $Q(6s6d\,{}^1D_2)$ |
|---|---|---|---|---|
| 5.00 | 0.81 | 5.45 | 2.74 | 1.21 |
| 6.00 | 0.89 | 4.95 | 2.54 | 1.79 |
| 7.00 | 1.23 | 4.07 | 2.41 | 2.25 |
| 8.35 | 1.79 | 3.69 | 1.87 | 2.21 |
| 9.00 | 1.17 | 3.59 | 1.57 | 1.96 |
| 10.00 | 0.70 | 3.53 | 1.51 | 2.01 |
| 11.44 | 0.55 | 3.39 | 1.44 | 2.28 |
| 15.00 | 0.48 | 2.99 | 1.28 | 2.13 |
| 20.00 | 0.36 | 2.74 | 0.90 | 1.89 |
| 30.00 | 0.38 | 2.46 | 0.51 | 1.50 |
| 36.67 | 0.38 | 2.33 | 0.37 | 1.29 |
| 41.44 | 0.38 | 2.24 | 0.31 | 1.15 |
| 50.00 | 0.35 | 2.00 | 0.24 | 0.97 |
| 60.00 | 0.31 | 1.78 | 0.19 | 0.81 |
| 80.00 | 0.27 | 1.44 | 0.13 | 0.62 |
| 100.00 | 0.23 | 1.22 | 0.10 | 0.50 |
| 200.00 | 0.14 | 0.69 | 0.043 | 0.25 |
| 400.00 | 0.08 | 0.37 | 0.018 | 0.125 |
| 600.00 | 0.05 | 0.25 | 0.012 | 0.083 |
| 897.60 | 0.03 | 0.16 | 0.008 | 0.056 |

culated cascade contribution. Chen and Gallagher have used the Bethe-Born theory to normalize their relative measurements at high energy. They used the value of the optical oscillator strength $f=1.59$ a.u. for the $6s^2\,{}^1S-6s6p\,{}^1P_1$ transition. This value is now known more accurately, $f=1.64$ a.u. [35]. We therefore have multiplied the cross-section values given by Chen and Gallagher by the ratio of the latter and former optical oscillator strengths. The excellent agreement between experiment and the CCC results gives credence to the CCC method and some assurance that the $Q(6s6p\,{}^1P_1)$ cross sections from these calculations are reliable. In Fig. 1(b), we compare these cross sections with

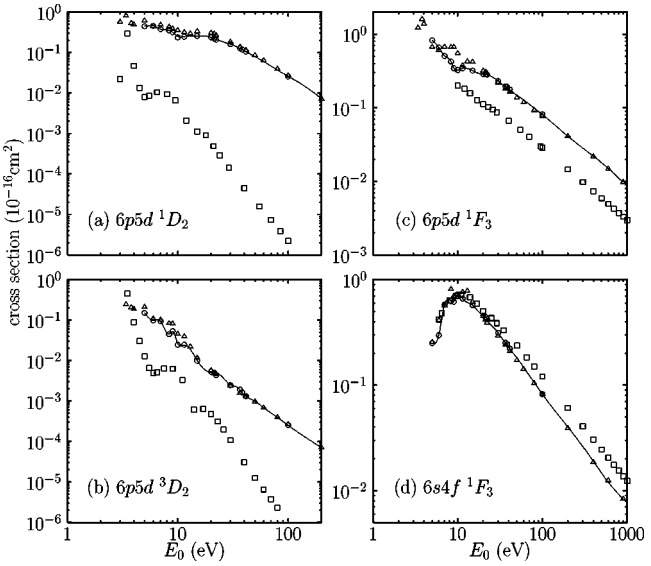


FIG. 5. Same as Fig. 4 except for (a) $6p5d\,{}^1D_2$, (b) $6p5d\,{}^3D_2$, (c) $6p5d\,{}^1F_3$, and (d) $6s4f\,{}^1F_3$ levels.

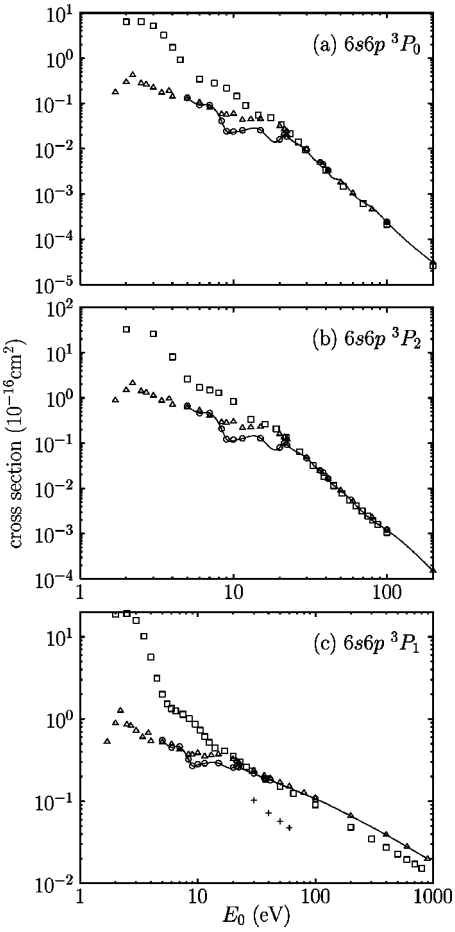


FIG. 6. Same as Fig. 4 except for the $6s6p\,{}^3P_{0,1,2}$ levels.

TABLE V. Recommended $Q(6p5d\,^1D_2)$, $Q(6p5d\,^1F_3)$, $Q(6s4f\,^1F_3)$, and $Q(6p5d\,^3D_2)$ values in units of $10^{-16}\,\mathrm{cm}^2$.

| $E_0$ (eV) | $Q(6p5d\,^1D_2)$ | $Q(6p5d\,^1F_3)$ | $Q(6s4f\,^1F_3)$ | $Q(6p5d\,^3D_2)$ |
|---|---|---|---|---|
| 5.00 | 0.446 | 0.826 | 0.249 | 0.150 |
| 6.00 | 0.456 | 0.661 | 0.297 | 0.098 |
| 7.00 | 0.376 | 0.506 | 0.580 | 0.093 |
| 8.35 | 0.355 | 0.424 | 0.626 | 0.045 |
| 9.00 | 0.319 | 0.345 | 0.617 | 0.053 |
| 10.00 | 0.249 | 0.322 | 0.718 | 0.026 |
| 11.44 | 0.246 | 0.344 | 0.661 | 0.024 |
| 15.00 | 0.256 | 0.320 | 0.571 | 0.010 |
| 20.00 | 0.238 | 0.287 | 0.457 | 0.005 |
| 30.00 | 0.161 | 0.231 | 0.314 | 0.0025 |
| 36.67 | 0.127 | 0.195 | 0.252 | 0.0019 |
| 41.44 | 0.105 | 0.177 | 0.221 | 0.0013 |
| 50.00 | 0.079 | 0.148 | 0.181 | 0.00098 |
| 60.00 | 0.060 | 0.128 | 0.147 | 0.00068 |
| 80.00 | 0.037 | 0.099 | 0.106 | 0.00039 |
| 100.00 | 0.026 | 0.081 | 0.082 | 0.00025 |
| 200.00 | 0.0072 | 0.041 | 0.04 | |
| 400.00 | 0.0009 | 0.022 | 0.019 | |
| 600.00 | 0.00025 | 0.015 | 0.012 | |
| 897.60 | 0.00017 | 0.0097 | 0.0083 | |

those obtained from Chen and Gallagher, $Q_{\mathrm{app}}(6s6p\,^1P_1)$, and the results obtained from other calculational methods. As can be seen from Fig. 1(b), the calculational methods converge at higher impact energies (above a few hundred eV) but only the CCC results can be considered reliable at intermediate and low impact energies. The set of recommended cross sections is given in Table II. The apparent cross sections are those of Chen and Gallagher, marginally renormalized by multiplication by 1.03 as discussed above. The ratio of $Q_{\mathrm{cascade}}/Q_{\mathrm{app}}$ has been evaluated using the CCC and CC(55) results. Both recommended cascade $Q_{\mathrm{cascade}}$ and direct $Q(6s6p\,^1P_1)$ cross sections have been obtained from the apparent cross sections with the utilization of the CCC $Q_{\mathrm{cascade}}/Q_{\mathrm{app}}$ ratio.

### B. Other inelastic-scattering channels

In all UFOMBT calculations except for the excitation of the $6s4f\,^1F_3$ and the $6p5d\,^1D_2$ levels, the 22 configurational basis set described in Zetner *et al.* [34] was used.

Apparent level excitation and electron impact excitation cross sections for the $6s7p\,^1P_1$ and $6s8p\,^1P_1$ levels, obtained from CCC, CC(55), and UFOMBT calculations, are shown in Figs. 2 and 3, respectively. No experimental data or other theoretical results are available for these excitation processes. The recommended cross sections are listed in Table III. These values correspond to the CCC results. No recommended cross sections are given below 5.0 eV since the present implementation of the CCC method is too computationally expensive to study resonance regions.

Electron impact excitation cross sections for the $5d^2\,^1S$ level and $^1D_2$ levels associated with the $6s5d$, $5d^2$, and $6s6d$ major configurations are given in Fig. 4. We did not include the very approximate $Q(6s5d\,^1D_2)$ values of Jensen *et al.* [16] in Fig. 4(b). No other results are available, and again we give our recommended cross sections based on the CCC calculations in Table IV.

Other important excitation channels are associated with the $6p5d\,^1D_2$, $6p5d\,^1F_3$, $6s4f\,^1F_3$, and $6p5d\,^3D_2$ levels. The theoretical results for these cross sections are shown in Fig. 5 and the recommended values are listed in Table V.

Excitations of triplet levels are given for $6s6p\,^3P_J$ ($J=0$, 1, and 2) and $6s5d\,^3D_J$ ($J=1$, 2, and 3). Only theoretical cross sections are available and they are shown in Figs. 6 and 7, respectively. The recommended values are summarized in Table VI.

Comparing CCC and UFOMBT results, we generally find good agreement at high incident electron energies. However, for a few transitions we observe substantial discrepancies even at high impact energies. For the $6p5d\,^1F_3$ state [Fig. 5(c)], this discrepancy is the result of the small but important difference in the CI mixing coefficients for the $nf6s\,^1F_3$ configuration. We find that the $nf6s\,^1F_3$ configuration contributes most to the ICS, specially at high energies. We gave preference to the CCC results in this case, because it is likely that the structure calculation performed in the UFOBT method has not converged for this state. Similarly, for the $6s5d\,^3D_2$ level [Fig. 7(c)] a small difference in the singlet-triplet mixing coefficient between $6s5d\,^3D_2$ and $6s5d\,^1D_2$ configurations leads to some differences between CCC and UFOMBT calculations at high energies.

The enormous difference between CCC and UFOMBT results for the $6p5d\,^1D_2$ and $6p5d\,^3D_2$ levels [Figs. 5(a) and 5(b)] has nothing to do with differences in the structure models but comes from the difference in the scattering calculations. In a first-order theory, such as UFOMBT, in the nonrelativistic approximation the excitation of both

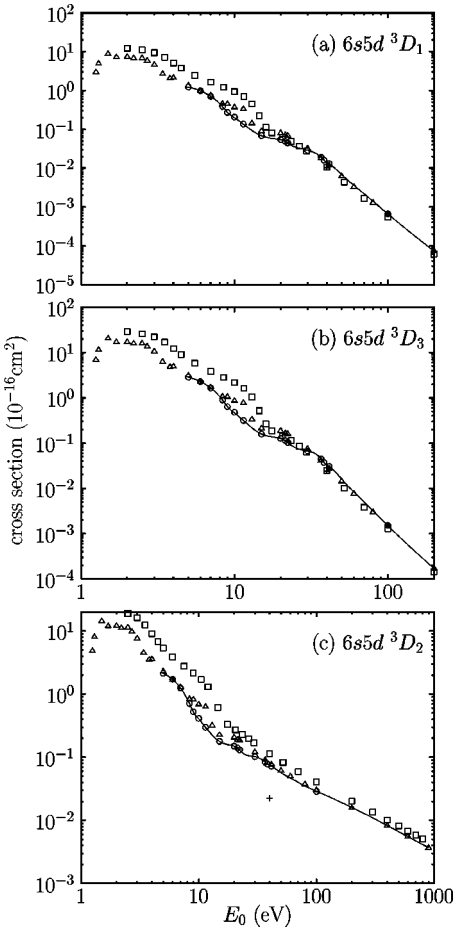


FIG. 7. Same as Fig. 4 except for the $6s5d\,^3D_{1,2,3}$ levels.

$6p5d\,^1D_2$ and $6p5d\,^3D_2$ levels from the $6s^2\,^1S$ ground state can occur by exchange scattering only. As the incident electron energy increases, the exchange scattering decreases, which leads to very small values of the excitation cross section. Account of relativistic corrections in UFOMBT does not change this situation because the singlet-triplet mixing in the ground state is negligible, while the singlet-triplet mixing for $6p5d\,^1D_2$ and $6p5d\,^3D_2$ levels brings contributions from exchange transitions only. On the other hand, in a close-coupling theory, excitation of the $6p5d\,^1D_2$ level (in the nonrelativistic approximation) can occur as a two- (or more) step process. Such processes, for example $6s^2\,^1S \rightarrow 6s5d\,^1D_2 \rightarrow 6p5d\,^1D_2$, can occur via direct scattering, which leads to significantly larger cross sections. The account of relativistic corrections for the $6p5d\,^3D_2$ level leads to significant increase of the cross section due to admixture of the singlet $6p5d\,^1D_2$ level, see Eq. (5h).

### C. Ionization

Total ionization ($Q^+ + Q^{++} + \cdots = Q_i$) and single ionization ($Q^+$) cross sections were measured by Dettmann and Karstensen [18] and total ionization ($Q_i$) by Vainshtein *et al.* [19]. The CCC results are available only for $Q^+$ (threshold for double ionization is at 15.2 eV). These results are shown in Fig. 8. It is clear that the CCC method substantially underestimates the experimental $Q^+$. At incident electron energies above 15 eV, this is related to the opening of the $5p^6$ shell. This process is not accounted for in the CCC model (which has inert inner shells). However, below the inner-shell ionization threshold, the CCC method should be able to account for all major ionization channels. Inclusion in the CCC calculations of $G$ states and other states with larger angular momentum will result in a larger ionization cross

TABLE VI. Recommended $Q(6s6p\,^3P_J)$ and $Q(6s5d\,^3D_J)$ values in units of $10^{-16}$ cm$^2$.

| | $Q(6s6p\,^3P_J)$ | | | $Q(6s5d\,^3D_J)$ | | |
|---|---|---|---|---|---|---|
| $E_0$ (eV) | $J=0$ | $J=1$ | $J=2$ | $J=1$ | $J=2$ | $J=3$ |
| 5.00 | 0.133 | 0.553 | 0.664 | 1.232 | 2.130 | 2.875 |
| 6.00 | 0.093 | 0.451 | 0.463 | 0.983 | 1.712 | 2.293 |
| 7.00 | 0.092 | 0.460 | 0.461 | 0.710 | 1.247 | 1.656 |
| 8.35 | 0.041 | 0.323 | 0.207 | 0.385 | 0.710 | 0.899 |
| 9.00 | 0.024 | 0.269 | 0.122 | 0.272 | 0.524 | 0.635 |
| 10.00 | 0.023 | 0.278 | 0.113 | 0.199 | 0.404 | 0.464 |
| 11.44 | 0.025 | 0.289 | 0.127 | 0.135 | 0.297 | 0.316 |
| 15.00 | 0.026 | 0.291 | 0.129 | 0.068 | 0.178 | 0.159 |
| 20.00 | 0.016 | 0.257 | 0.080 | 0.054 | 0.150 | 0.127 |
| 30.00 | 0.009 | 0.219 | 0.043 | 0.029 | 0.102 | 0.067 |
| 36.67 | 0.005 | 0.192 | 0.025 | 0.019 | 0.084 | 0.045 |
| 41.44 | 0.003 | 0.180 | 0.016 | 0.013 | 0.072 | 0.031 |
| 50.00 | 0.002 | 0.161 | 0.009 | 0.0068 | 0.057 | 0.016 |
| 60.00 | 0.001 | 0.145 | 0.005 | 0.0036 | 0.047 | 0.0084 |
| 80.00 | 0.0005 | 0.122 | 0.002 | 0.0014 | 0.035 | 0.0032 |
| 100.00 | 0.00024 | 0.107 | 0.0012 | 0.0007 | 0.029 | 0.0015 |
| 200.00 | | 0.066 | | | 0.016 | |
| 400.00 | | 0.039 | | | 0.0083 | |
| 600.00 | | 0.028 | | | 0.0055 | |
| 897.60 | | 0.020 | | | 0.0037 | |

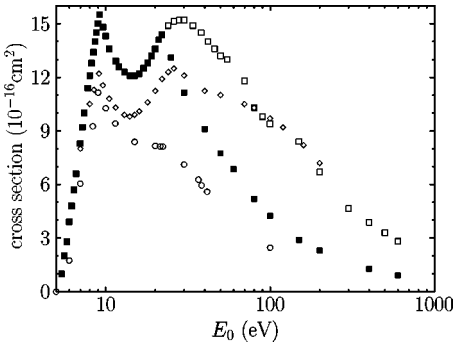


FIG. 8. Ionization cross sections: ○, CCC ($Q^+$); □, ($Q_i$), ■, ($Q^+$), Dettmann and Karstensen [18]; and ◇, ($Q_i$), Vainshtein *et al.* [19].

section. The convergence in the TICS, with increasing target-space orbital angular momentum, is relatively fast [36] and we estimate that CCC results should converge to values 10–15 % larger than the present results. This correction of the CCC results would bring them into very good agreement with measurements of TICS by Vainshtein *et al.* [19] in the region of the first TICS maximum. The discrepancy between the experimental results and between the experimental and the theoretical results in this energy range makes it impossible for us to present a reliable set of recommended TICS values. More accurate theoretical calculations and/or new independent measurements are required to draw any definite conclusions. For the time being, we arbitrarily renormalized the results of Dettmann and Karstensen [18] at the first maximum to the value of $1.3\times10^{-15}$ cm$^2$. These renormalized values are listed in Table VII.

### D. Elastic scattering, momentum transfer, and total scattering

Elastic scattering and momentum transfer cross sections are available from a number of calculations. They are shown

TABLE VII. Estimate of ionization cross section $Q_{\rm ion}$ and $Q^+$ values in units of $10^{-16}$ cm$^2$.

| $E_0$ (eV) | $Q_{\rm ion}$ | $Q^+$ |
|---|---|---|
| 5.40 | 0.8 | 0.8 |
| 6.00 | 3.3 | 3.3 |
| 7.00 | 7.0 | 7.00 |
| 8.00 | 10.1 | 10.1 |
| 9.00 | 12.6 | 12.6 |
| 10.00 | 12.0 | 12.0 |
| 12.00 | 10.6 | 10.6 |
| 15.00 | 10.2 | 10.2 |
| 20.00 | 11.4 | 11.4 |
| 30.00 | 12.8 | 9.3 |
| 40.00 | 12.0 | 7.6 |
| 50.00 | 11.1 | 6.5 |
| 80.00 | 8.6 | 4.3 |
| 100.00 | 7.9 | 3.6 |
| 150.00 | 7.1 | 2.4 |
| 200.00 | 5.6 | 1.9 |
| 400.00 | 3.3 | 1.1 |
| 600.00 | 2.4 | 0.8 |

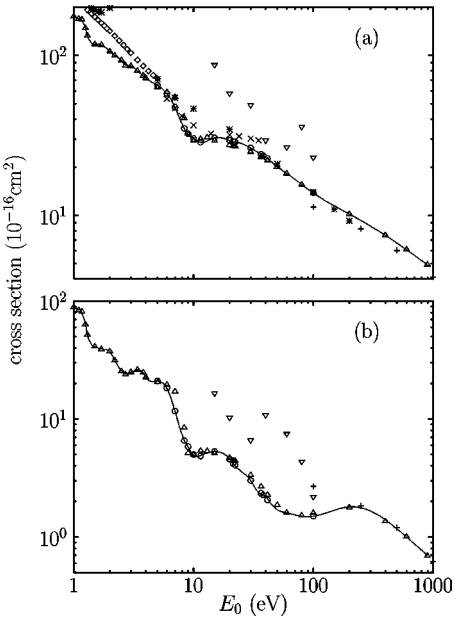


FIG. 9. Integral elastic (a) and momentum transfer (b) cross sections: ○, CCC; △, CC(55); +, Gregory and Fink [21]; ×, CC(2), Fabrikant [22]; ∇, Szmytkowski and Sienkiewicz [25]; ◇, Yuan and Zhang [23];*, Kelemen *et al.* [26]. The solid line represents our recommended values.

TABLE VIII. Recommended $Q_{\rm elas}$, $Q_M$, and $Q_{\rm tot}$ values in units of $10^{-16}$ cm$^2$.

| $E_0$ (eV) | $Q_{\rm elas}$ | $Q_M$ | $Q_{\rm tot}$ |
|---|---|---|---|
| 1.00 | 175.3 | 88.8 | 175.3 |
| 1.50 | 117.5 | 41.1 | 162.4 |
| 2.00 | 106.1 | 37.4 | 148.7 |
| 2.50 | 93.4 | 25.4 | 142.0 |
| 3.00 | 86.0 | 24.9 | 130.5 |
| 4.00 | 72.1 | 22.5 | 122.2 |
| 5.00 | 65.1 | 21.0 | 120.0 |
| 6.00 | 57.8 | 18.2 | 117.3 |
| 7.00 | 47.5 | 11.7 | 112.8 |
| 8.35 | 35.0 | 6.6 | 101.3 |
| 9.00 | 32.3 | 5.8 | 97.2 |
| 10.00 | 30.2 | 4.9 | 94.8 |
| 11.44 | 28.6 | 4.9 | 92.0 |
| 15.00 | 30.6 | 5.3 | 91.7 |
| 20.00 | 29.4 | 4.6 | 87.4 |
| 30.00 | 26.4 | 3.0 | 77.8 |
| 41.44 | 22.7 | 2.1 | 67.2 |
| 50.00 | 20.1 | 1.7 | 60.0 |
| 60.00 | 18.3 | 1.6 | 55.0 |
| 80.00 | 15.6 | 1.5 | 46.0 |
| 100.00 | 13.8 | 1.5 | 39.9 |
| 200.00 | 10.2 | 1.8 | 24.7 |
| 400.00 | 7.5 | 1.4 | 15.9 |
| 600.00 | 6.1 | 1.0 | 12.0 |
| 897.60 | 4.9 | 0.7 | 9.1 |

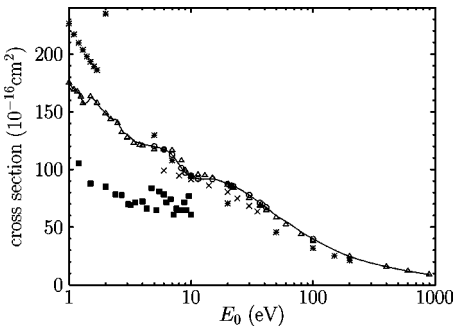


FIG. 10. Total electron scattering cross sections: ○, CCC; △, CC(55); ×, CC(2), Fabrikant [22];*, Kelemen *et al.* [26]; ■, Romanyuk *et al.* [20]. The solid line represents our recommended values.

in Fig. 9. Our recommended values are given in Table VIII, where we have also included the recommended total electron scattering cross sections, see Fig. 10, based mainly on the CCC results. At low energies, the experimental results of Romanyuk *et al.* [20] are in poor agreement with our results as well as with the results of all other calculations. Hence we suppose that the present theoretical results are more accurate than the experimental ones.

## IV. CONCLUSIONS

We have presented a recommended set of integrated cross sections for electron scattering by the ground state of barium. For most of the transitions presented here, no previous experimental or theoretical data are available. We expect our results to be useful in practical applications and will stimulate further experimental and theoretical effort to continue to improve the cross-section data set.

## ACKNOWLEDGMENTS

We are grateful to V. Kelemen and A. Stauffer for communicating their data in electronic form. Support of the Australian Research Council and the Flinders University of South Australia, the National Science Foundation, and the National Aeronautic and Space Administration is acknowledged. We are also indebted to the South Australian Center for High Performance Computing and Communications. The work at the Los Alamos National Laboratory has been performed under the auspices of the U.S. Department of Energy and has been partially supported by the Electric Power Research Institute.

[1] R. P. Mildren, D. J. W. Brown, R. J. Carman, and J. A. Piper, Opt. Commun. **120**, 112 (1995).
[2] R. P. Mildren, D. J. W. Brown, and J. A. Piper, IEEE J. Quantum Electron. **33**, 1717 (1997).
[3] R. P. Mildren, D. J. W. Brown, and J. A. Piper, J. Appl. Phys. **82**, 2039 (1997).
[4] R. P. Mildren, D. J. W. Brown, and J. A. Piper, Opt. Commun. **137**, 299 (1997).
[5] A. K. Bhattacharya, J. Appl. Phys. **137**, 299 (1997).
[6] C. M. Yang and A. E. Rodrigez, Wright Laboratory, Report TR-92-006, Wright Patterson AFB, Ohio March, 1992.
[7] E. M. Wescott, H. C. Stenbaek-Nielsen, J. J. Hallinan, C. S. Deehr, G. J. Romick, S. V. Olson, J. G. Roederer, and R. Sydora, Geophys. Res. Lett. **7**, 1037 (1980).
[8] D. J. Simons, M. B. Pongratz, G. M. Smith, and G. E. Barasch, J. Geophys. Res. **86**, 1576 (1981).
[9] D. Winske, J. Geophys. Res. **93**, 2539 (1988).
[10] S. C. Chapman, J. Geophys. Res. **94**, 227 (1989).
[11] R. W. Shuk and E. P. Szuszgzewiez, J. Geophys. Res. **96**, 1337 (1991).
[12] E. M. Wescott *et al.*, J. Geophys. Res. **98**, 3711 (1993).
[13] S. T. Chen and A. Gallagher, Phys. Rev. A **14**, 593 (1976).
[14] S. Trajmar and J. C. Nickel, Adv. At. Mol. Phys. **30**, 45 (1992).
[15] D. V. Fursa and I. Bray, Phys. Rev. A **59**, 282 (1999).
[16] S. Jensen, D. Register, and S. Trajmar, J. Phys. B **11**, 2367 (1978).
[17] S. Wang, S. Trajmar, and P. W. Zetner, J. Phys. B **27**, 1613 (1994).
[18] J. Dettmann and F. Karstensen, J. Phys. B **15**, 287 (1982).
[19] L. A. Vainshtein, V. I. Ochcur, V. I. Rakhovskii, and A. M. Stepanov, Zh. Eksp. Teor. Fiz. **61**, 511 (1971) [Sov. Phys. JETP **34**, 271 (1972)].
[20] N. I. Romanyuk, O. B. Shpenik, and I. P. Zapesochny, Pis'ma Zh. Eksp. Teor. Fiz. **32**, 472 (1980) [JETP **32**, 452 (1980)]
[21] D. Gregory and M. Fink, At. Data Nucl. Data Tables **14**, 39 (1974).
[22] I. I. Fabrikant, J. Phys. B **13**, 603 (1980).
[23] J. Yuan and Z. Zhang, Phys. Rev. A **42**, 5363 (1990).
[24] J. Yuan and Z. Zhang, Phys. Lett. A **168**, 291 (1992).
[25] R. Szmytkowski and J. E. Sienkiewicz, Phys. Rev. A **50**, 4007 (1994).
[26] V. I. Kelemen, E. Y. Remeta, and E. P. Sabad, J. Phys. B **28**, 1527 (1995).
[27] G. F. Gribakin, B. V. Gul'tsev, V. K. Ivanov, M. Y. Kuchiev, and A. R. Tancic, Phys. Lett. A **164**, 73 (1992).
[28] R. E. H. Clark, J. Abdallah, Jr., G. Csanak, and S. P. Kramer, Phys. Rev. A **40**, 2935 (1989).
[29] R. Srivastava, T. Zuo, R. P. McEachran, and A. D. Stauffer, J. Phys. B **25**, 3709 (1992).
[30] R. Srivastava, R. P. McEachran, and A. D. Stauffer, J. Phys. B **25**, 4033 (1992).
[31] D. V. Fursa and I. Bray, Phys. Rev. A **57**, R3150 (1998).
[32] D. V. Fursa and I. Bray, J. Phys. B **30**, 5895 (1997).
[33] H. E. Saraph, Comput. Phys. Commun. **3**, 256 (1972).
[34] P. W. Zetner, S. Trajmar, S. Wang, I. Kanik, G. Csanak, R. E. Clark, J. Abdallah, and J. C. Nickel, J. Phys. B **30**, 5317 (1997).
[35] C. W. Bauschlicher, Jr., R. L. Jaffe, S. R. Langhoff, F. G. Mascarello, and H. Partridge, J. Phys. B **18**, 2147 (1985).
[36] I. Bray, Phys. Rev. Lett. **73**, 1088 (1994).
[37] C. E. Moore, *Atomic Energy Levels*, Natl. Bur. Stand. Circ. No. 467, Vol. III (U.S. GPO, Washington, D.C., 1949).
[38] H. P. Palenius, Phys. Lett. **56A**, 451 (1976).